

Supporting Information

Unexpected Solute Occupancy and Anisotropic Polarizability in Lewis Basic Solutions

Siyan Gao¹, Yongli Huang^{1,*}, Xi Zhang^{2,*}, Chang Q Sun³

1 Structure optimization

We adopted three possible Y^+ positions, central-tetrahedron position, above-triangle position, and in-triangle position, as shown in Figure S1. The central-tetrahedron position means that Y^+ ion is located at the center of a water tetrahedron unit. The Y^+ ion has six nearest water neighbors and the distance is the lattice constant a . The above-triangle position means that Y^+ ion is located above three oxygen atoms forming a triangle in a plane. The distance between Y^+ ion and oxygen is smaller than a . The in-triangle position means that Y^+ ion is located in the center of oxygen atoms-triangle in a plane. Y^+ ion has three nearest neighbors and the distance is the smallest. It can be predicted the Y^+ ion will induce the larger lattice distortion and instability when it get closer to water molecule. We performed structural optimizations of these aqueous solution models. As predicted, the in-triangle position is the most unstable, and the above-triangle position the second. The total energy for central-tetrahedron position, above-triangle position, and in-triangle position are -133395.04 eV, -133392.11 eV, and -133388.85 eV, respectively. The OH^- ion was

¹ School of Materials Science and Engineering, Xiangtan University, Hunan 411105, China (siyangaoxtu@163.com; huangyongli@xtu.edu.cn)

² Institute of Nanosurface Science and Engineering, Shenzhen University, Shenzhen 518060, China; (zh0005xi@szu.edu.cn)

³ NOVITAS, School of Electrical and Electronic Engineering, Nanyang Technological University, Singapore 639798, Singapore; (ecqsun@ntu.edu.sg)

not induced additionally but just changed from a water molecule in the crystal structure.

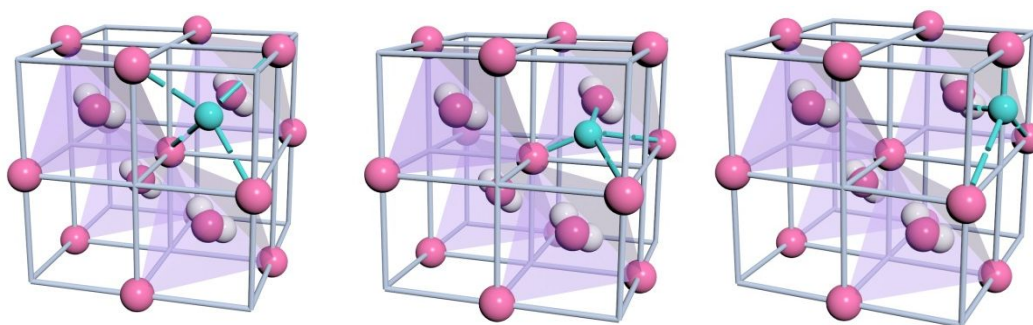


Figure S1. Three different positions of Y^+ ion. (a) Central-tetrahedron position; (b) Above-triangle position; (c) In-triangle position.

2 Vibrational mode

The vibration mode shift positions are confirmed through the same frequency vibrational mode in the frequency ranges of $\omega_L < 400 \text{ cm}^{-1}$ and $\omega_H > 3000 \text{ cm}^{-1}$. Figure S2 shows specific vibrational modes of hydrogen bond segments, O:H nonbond and H-O bond, at different frequencies. The frequency of 253 cm^{-1} shows the O:H stretching mode and the frequency of 832 cm^{-1} is the O:H bending mode. For the higher frequency, the frequencies of 3087 cm^{-1} and 3294 cm^{-1} are H-O symmetric and asymmetric stretching modes, respectively.

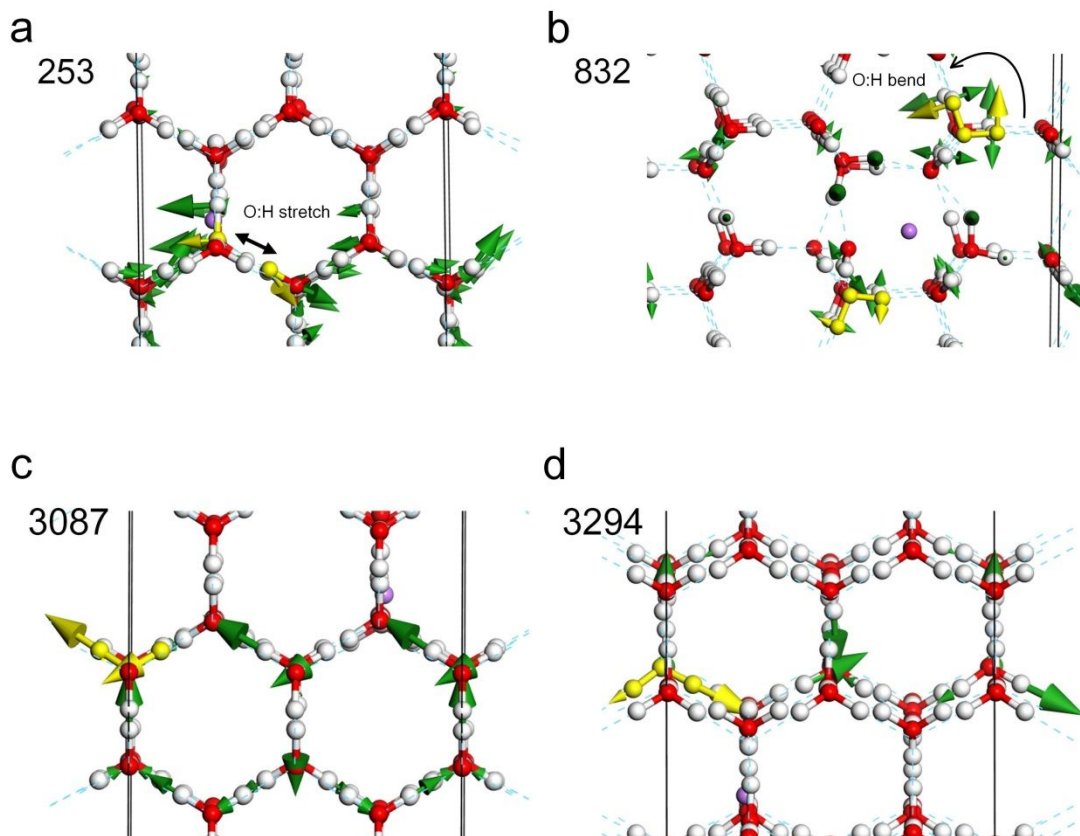


Figure S2. (a) The stretching mode of O:H at 253 cm⁻¹. (b) The bending mode at 832 cm⁻¹. (c) The stretching mode of H-O at 3087 cm⁻¹ (symmetric stretching) and 3294 cm⁻¹(asymmetric stretching), respectively.

3 MD calculation

We further employed molecular dynamics (MD) calculation to compute the power spectrum of water containing OH⁻ (supporting information). We carried out MD calculations using Forcite's package with *ab initio* optimized forcefield CompassII¹. The unit cell consisted of 64 water molecules and an OH⁻ hydroxide. The electronic structure was dynamically relaxed during 10 ps (20000 steps) in the NVT ensemble. The temperature was set as 298K and the thermostat was applied by Mass GGM method. The equilibrium structures were gained after 10 ps at the time step of 0.5 fs. Further, we computed the power spectra through the Fourier transformation of the velocity autocorrelation function², $Cor(t)$, $I(\omega) = 2 \int_0^\infty Cor(v(t)) \cos(\omega t) dt$ employing velocity data of all atoms in the dynamic system.

Figure S3 shows the MD-derived power spectrum of pure water and OH⁻ solution. Figure S4 compares the differential spectra (OH⁻ solution subtracted by water). Compared to DFT-derived vibration spectra, the MD-derived power spectrum has the same frequency shifts of O-H and O:H bonds. The fluctuation was caused by the temperature of 298K applied in MD. The results reveal that the O: \rightleftharpoons :O repulsion lengthen the opposing H-O bond but shorten the subsequent O:H cooperatively.

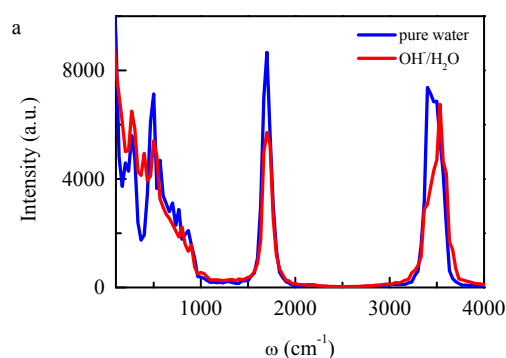


Figure S3. The MD-derived power spectrum of pure water and OH⁻ solution.

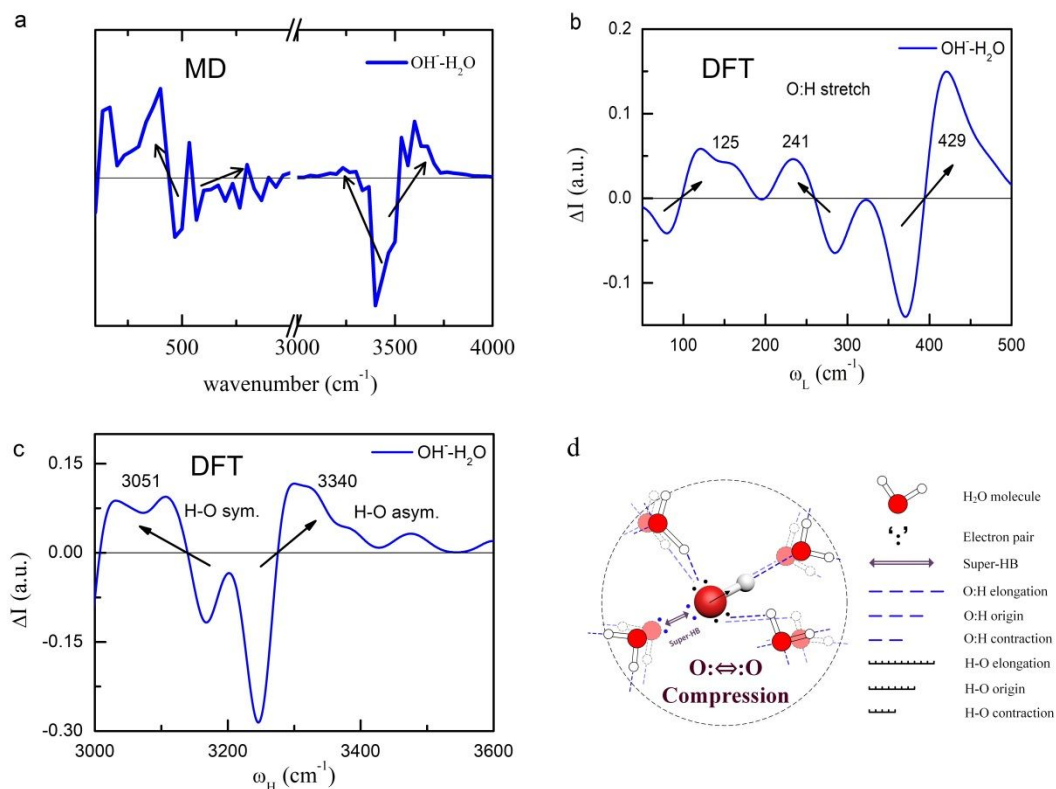


Figure S4. The differential spectra (OH⁻ solution subtracted by water) of (a)

MD-derived power spectrum and DFT-derived vibration spectra for (b) ω_L (50 ~ 600 cm^{-1}) and (c) ω_H (3100 ~ 3600 cm^{-1}) between the $\text{OH}^-/\text{H}_2\text{O}$ solutions and pure water.

(d) The diagram of the first hydration shell of OH^- -contained water.

References

1. Sun, H.; Jin, Z.; Yang, C.; Akkermans, R. L.; Robertson, S. H.; Spenley, N. A.; Miller, S.; Todd, S. M., COMPASS II: extended coverage for polymer and drug-like molecule databases. *Journal of molecular modeling* **2016**, 22 (2), 47.
2. (a) Kang, D.; Dai, J.; Hou, Y.; Yuan, J., Structure and vibrational spectra of small water clusters from first principles simulations. *The Journal of Chemical Physics* **2010**, 133 (1), 014302;
(b) Sun, C. Q.; Zhang, X.; Zheng, W., The hidden force opposing ice compression. *Chemical Science* **2012**, 3 (5), 1455-1460.